

NaCuMoO₄(OH) as a Candidate Frustrated J_1 - J_2 Chain Quantum Magnet

Kazuhiro Nawa^{1,*}, Yoshihiko Okamoto^{1,†}, Akira Matsuo¹, Koichi Kindo¹, Yoko Kitahara², Syota Yoshida², Shohei Ikeda², Shigeo Hara³, Takahiro Sakurai³, Susumu Okubo⁴, Hitoshi Ohta⁴, and Zenji Hiroi¹

¹*Institute for Solid State Physics, The University of Tokyo, Kashiwa, Chiba 277-8581, Japan*

²*Graduate School of Science, Kobe University, Nada, Kobe 657-8501, Japan*

³*Center for Supports to Research and Education Activities, Kobe University, Nada, Kobe 657-8501, Japan*

⁴*Molecular Photoscience Research Center, Kobe University, Nada, Kobe 657-8501, Japan*

(Dated: June 20, 2021)

In a frustrated J_1 - J_2 chain with the nearest-neighbor ferromagnetic interaction J_1 and the next-nearest-neighbor antiferromagnetic interaction J_2 , novel magnetic states such as a spin-nematic state are theoretically expected. However, they have been rarely examined in experiments because of the difficulty in obtaining suitable model compounds. We show here that the quasi-one-dimensional antiferromagnet NaCuMoO₄(OH), which comprises edge-sharing CuO₂ chains, is a good candidate J_1 - J_2 chain antiferromagnet. The exchange interactions are estimated as $J_1 = -51$ K and $J_2 = 36$ K by comparing the magnetic susceptibility, heat capacity, and magnetization data with the data obtained using calculations by the exact diagonalization method. High-field magnetization measurements at 1.3 K show a saturation above 26 T with little evidence of a spin nematic state expected just below the saturation field, which is probably due to smearing effects caused by thermal fluctuations and the polycrystalline nature of the sample.

Low-dimensional quantum spin systems with geometrical frustration and/or competing magnetic interactions have attracted much attention in the field of magnetism. Low dimensionality, quantum fluctuations, and frustration are three ingredients that may effectively suppress conventional magnetic order and lead us to unconventional magnetic order or exotic ground states such as a quantum spin liquid[1, 2].

A frustrated J_1 - J_2 chain of spin 1/2 defined as

$$\mathcal{H} = J_1 \sum_l \mathbf{s}_l \cdot \mathbf{s}_{l+1} + J_2 \sum_l \mathbf{s}_l \cdot \mathbf{s}_{l+2} - h \sum_l s_l^z \quad (1)$$

provides us with an interesting example: the competition between the nearest-neighbor (NN) ferromagnetic interaction J_1 and the next-nearest-neighbor (NNN) antiferromagnetic interaction J_2 causes various quantum states in magnetic fields h [3–7]. Realized in low fields is a long-range order of vector chirality defined as $(\mathbf{s}_l \times \mathbf{s}_{l+n})_z$ ($n = 1, 2$). As the field increases, spin correlations change markedly because bound magnon pairs are stabilized by ferromagnetic J_1 . The bound magnon pairs form a spin density wave (SDW) in medium fields, whereas, in high fields just below the saturation of magnetization, they exhibit Bose–Einstein condensation into quantum multipolar states[8–11]. One of the multipolar states expected just below the saturation is a quadrupolar state of magnon pairs called a spin nematic state, analogous to nematic liquid crystals.

To explore these quantum states theoretically predicted for the frustrated J_1 - J_2 chain, many experimental studies have been performed on quasi-1D compounds

TABLE I. Candidate compounds for the J_1 - J_2 chain system. Listed are the nearest-neighbor intrachain interaction J_1 , the next-nearest-neighbor interaction J_2 , the bond angles of Cu-O-Cu paths for J_1 , the antiferromagnetic transition temperature at zero field T_N , and the saturation field H_s .

Compound	J_1, J_2 (K)	\angle Cu-O-Cu (deg)	T_N (K)	H_s (T)
Li ₂ ZrCuO ₄ [12, 13]	-151, 35	94.1	6.4	-
Rb ₂ Cu ₂ Mo ₃ O ₁₂ [14, 15]	-138, 51	89.9, 101.8 91.9, 101.1	< 2	14
PbCuSO ₄ (OH) ₂ [16–18]	-100, 36	91.2, 94.3	2.8	5.4
LiCuSbO ₄ [19]	-75, 34	89.8, 95.0 92.0, 96.8	< 0.1	12
LiCu ₂ O ₂ [20–22]	-69, 43	92.2, 92.5	22.3	110
LiCuVO ₄ [23–31]	-19, 44	95.0	2.1	44.4
NaCuMoO ₄ (OH)	-51, 36	92.0, 103.6	0.59	26

such as Li₂ZrCuO₄[12, 13], Rb₂Cu₂Mo₃O₁₂[14, 15], PbCu(SO₄)(OH)₂[16–18], LiCuSbO₄[19], LiCu₂O₂[20–22], and LiCuVO₄[23–31], the key parameters of which are listed in Table I. These compounds commonly have edge-sharing CuO₂ chains made of CuO₆ octahedra. NN Cu spins are magnetically coupled with each other through two superexchange Cu–O–Cu paths with approximately 90° bond angles, while NNN Cu spins are coupled through two super-superexchange Cu–O–O–Cu paths. Thus, according to the Goodenough–Kanamori rule, J_1 should be ferromagnetic while J_2 can be antiferromagnetic. This is in fact the case for these candidate compounds, which causes frustration in the J_1 - J_2 chains.

Among these compounds, the most often studied is LiCuVO₄ with $J_1 = -19$ K and $J_2 = 44$ K[25]. It has been shown using large single crystals that LiCuVO₄ exhibits an incommensurate helical order at low fields[25–29], which may be a 3D analogue of the vector chirality

* knawa@issp.u-tokyo.ac.jp

† Present address: Department of Applied Physics, Graduate School of Engineering, Nagoya University, Chikusa, Nagoya 464-8603, Japan

order in the J_1 - J_2 chain, and a longitudinal SDW order at intermediate fields[26–29]. Furthermore, a spin nematic phase, a 3D analogue of the spin nematic state, has been suggested slightly below the saturation field of 44.4 T at $H \parallel c$, where the magnetization shows a linear field dependence[30]. However, the presence of the spin nematic phase is still unclear because of the high saturation field. Only NMR experiments were performed around the saturation, which revealed that the majority of magnetic moments were already saturated above 41.4 T, where the spin nematic phase was suggested from magnetization measurements. This discrepancy is likely due to crystal defects such as Li deficiency[31]. The other candidate compounds thus far studied also have some problems, such as disorder effects and the lack of large single crystals. Thus, an alternative compound is required for further experimental study of the J_1 - J_2 chain.

Here, we show that $\text{NaCuMoO}_4(\text{OH})$ is a good candidate compound that meets various experimental requirements. $\text{NaCuMoO}_4(\text{OH})$ was first prepared hydrothermally by Moini et al. in 1986 [32]. It crystallizes in an orthorhombic structure with the space group $Pnma$, which is isomorphous with that of the natural mineral Descloizite $\text{PbZnVO}_4(\text{OH})$ [33]. As shown in Fig. 1(a), there is a CuO_2 chain that may represent a J_1 - J_2 chain, similar to that observed in related compounds. We discover that $\text{NaCuMoO}_4(\text{OH})$ is a quasi-1D frustrated antiferromagnet with $J_1 = -51$ K, $J_2 = 36$ K, and $T_N = 0.59$ K. In addition, we show that the reasonably low saturation field of 26 T of this compound makes it promising for investigating an exotic spin nematic phase expected in the J_1 - J_2 chain system.

A polycrystalline sample of $\text{NaCuMoO}_4(\text{OH})$ was synthesized by the hydrothermal method. First, 3.807 g of 5 M NaOH aqueous solution (16.0 mmol of NaOH) was diluted by adding water to a volume of 10 ml. Then, 1.155 g of MoO_3 (8.0 mmol) and 0.8315 g of $\text{CuSO}_4 \cdot 5\text{H}_2\text{O}$ (3.3 mmol) were added. The mixed solution was put in a Teflon beaker of 30 ml volume, placed in a stainless steel autoclave, and heated at 240 °C for 48 h. An aggregate of small yellowish green crystals having a rod-like shape and a typical size of $0.1 \times 0.1 \times 0.2 \text{ mm}^3$ [inset of Fig. 1(b)] was obtained. The crystals were filtered, washed with water and ethanol, and dried at room temperature. To estimate the lattice contribution in heat capacity, a nonmagnetic analogue $\text{NaZnMoO}_4(\text{OH})$ was also prepared in a similar way.

Sample characterization was performed by powder X-ray diffraction (XRD) analysis using $\text{Cu } K_\alpha$ radiation (RINT-2000, Rigaku), by chemical analysis using inductively coupled plasma spectrometry (JY138KH, Horiba), and by thermal gravimetry (TG-DTA2020SAH, Bruker AXS). A powder XRD pattern from crashed crystals is shown in Fig. 1(b). In a whole powder pattern fitting using a program PDXL (Rigaku), all the peaks are indexed to reflections allowed for the space group $Pnma$ with the lattice constants $a = 7.7338(3)$ Å, $b = 5.9678(2)$ Å, and $c = 9.5091(3)$ Å, which are close to those previ-

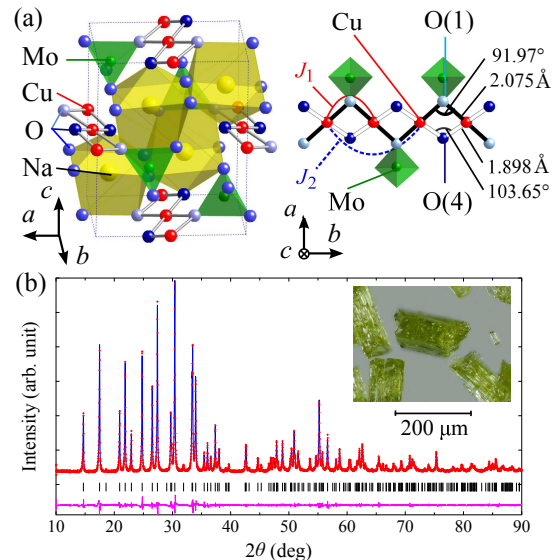


FIG. 1. (Color online) (a) Crystal structure of $\text{NaCuMoO}_4(\text{OH})$ (left) and a local environment around a CuO_2 chain (right) based on the structural parameters reported in Ref. 32. (b) Observed (red cross) and calculated (blue curve) powder XRD patterns ($\text{Cu } K_{\alpha_1}$ radiation) of a polycrystalline sample of $\text{NaCuMoO}_4(\text{OH})$. Additional contributions from $\text{Cu } K_{\alpha_2}$ radiation have been analytically removed. The positions of reflections and the difference in intensity between the observed and calculated patterns are indicated by vertical black lines and a magenta curve at the bottom, respectively. The inset shows a photograph of a small single crystal of $\text{NaCuMoO}_4(\text{OH})$.

ously reported: $a = 7.726(2)$ Å, $b = 5.968(2)$ Å, and $c = 9.495(3)$ Å[32]. The chemical compositions of Na, Mo, and Cu are 8.3(1), 23.6(1), and 35.3(2) wt%, respectively, which are close to the stoichiometric compositions of 8.7, 24.1, and 36.4 wt%; the small deviation may be due to the inclusion of small amounts of byproducts. A dehydration reaction with a weight loss of 3.3(1)% was observed above 350 °C, which means that nearly half mol of H_2O has been lost as expected from the chemical composition. Thus, we have successfully obtained $\text{NaCuMoO}_4(\text{OH})$ for detailed characterizations of its magnetic properties.

Magnetic susceptibility was measured in a SQUID magnetometer (MPMS, Quantum Design), and magnetization was measured up to 50 T in a pulse magnet at the Ultra High Magnetic Field Laboratory of the Institute for Solid State Physics at the University of Tokyo[34]. Heat capacity was measured by the relaxation method (PPMS, Quantum Design). The g factor of the paramagnetic state was estimated by multifrequency high-field ESR measurements up to 520 GHz at Kobe University[35] instead of by conventional X-band ESR measurements. Heat capacity measurements were performed on a thin pellet of a powdered sample, and all the other measurements were performed on an aggregate of single crystals.

The temperature dependence of magnetic susceptibility is shown in Fig. 2. No anomaly indicative of a long-

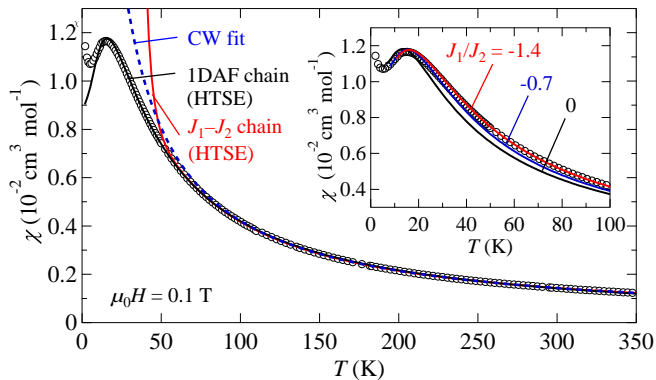


FIG. 2. (Color online) Temperature dependences of magnetic susceptibility. The blue dashed curves represent a Curie–Weiss (CW) fit, and the black and red solid curves represent fits to calculations based on the high-temperature series expansion (HTSE) for uniform 1D antiferromagnetic (1DAF)[36] and frustrated J_1 – J_2 chains[38], respectively. The inset shows the magnetic susceptibility compared with these obtained using calculations by the exact diagonalization method for J_1 – J_2 chains with $J_1/J_2 = -1.4$ (red curve), -0.7 (blue curve), and 0 (black curve), where the g factor and temperature-independent contribution are fixed to $g = 2.11$ determined from the ESR measurement and $\chi_0 = 1.2 \times 10^{-5} \text{ cm}^3 \text{ mol}^{-1}$ from the HTSE fit, respectively.

range order is observed above 2 K, while a broad peak is observed at 14 K, indicating the presence of a 1D antiferromagnetic correlation. The magnetic susceptibility in the range of 150–350 K is fitted to the sum of a Curie–Weiss contribution and a temperature-independent contribution χ_0 ,

$$\chi(T) = \frac{Ng^2\mu_B^2 S(S+1)}{3k_B(T-\theta)} + \chi_0, \quad (2)$$

where g is the Lande g factor, μ_B is the Bohr magneton, k_B is the Boltzmann constant, and θ is the Weiss temperature. The fitting shown by the dotted line in Fig. 2 yields $\theta = -5.0(5)$ K, $g = 2.18(1)$, and $\chi_0 = -2.5(4) \times 10^{-5} \text{ cm}^3 \text{ mol}^{-1}$.

χ in the range of 8–350 K is alternatively fitted to a 1D antiferromagnetic (1DAF) chain model[36]. The calculated curve well reproduces χ , particularly the broad peak at 14 K, and yields $J_{1\text{DAF}} = 24.4(1)$ K, $g = 2.30(1)$, and $\chi_0 = -1.67(1) \times 10^{-4} \text{ cm}^3 \text{ mol}^{-1}$. However, this fitting suffers from the following two inconsistencies. First, g of 2.30 is too large for the powder average for Cu^{2+} ions, typically 2.1–2.2, and χ_0 is too small compared with the diamagnetic susceptibility from core electrons, $\chi_{\text{dia}} = -8.3 \times 10^{-5} \text{ cm}^3 \text{ mol}^{-1}$; χ_0 must be larger than χ_{dia} since there must be an additional positive contribution from the Van Vleck paramagnetism. Second, the Weiss temperature expected in the mean field theory is $\theta = -J_{1\text{DAF}}/2 = -12$ K in the 1DAF chain, which is significantly different from $\theta = -5.0$ K from the Curie–Weiss fit. Similar discrepancies have been observed in

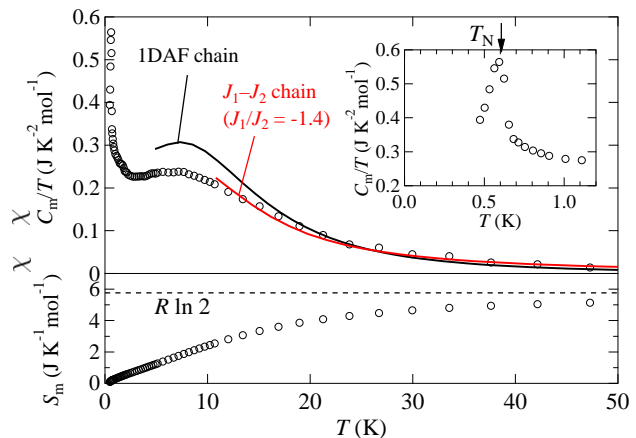


FIG. 3. (Color online) Temperature dependences of magnetic heat capacity divided by temperature and magnetic entropy. The black and red curves show heat capacities for a uniform 1DAF chain with $J = 24.4$ K and a frustrated J_1 – J_2 chain with $J_1 = -51$ K and $J_2 = 36$ K ($J_1/J_2 = -1.4$) calculated by the exact diagonalization method, respectively. The inset expands the low-temperature part, where a sharp anomaly indicates a phase transition.

LiCuVO_4 : a fit to the 1DAF chain model gives a larger g than that determined by ESR measurements[37] and a smaller $-J_{1\text{DAF}}/2$ than θ for the Curie–Weiss fit[25, 37]. Thus, there must be additional ferromagnetic couplings in these compounds.

Provided that there are two magnetic interactions, ferromagnetic J_1 and antiferromagnetic J_2 , in $\text{NaCuMoO}_4(\text{OH})$, we have determined J_1 and J_2 by analyzing χ more elaborately on the bases of simulations by the high-temperature series expansion (HTSE)[38] and exact diagonalization (ED) method. First, we have determined the g factor by ESR experiments. Absorption lines observed at 173 K at frequencies between 200 and 520 GHz were well reproduced by single Lorentzian curves with linewidths of about 2 T. g is estimated to be 2.11(2) from a linear relation between the resonant frequency and the field.

Fitting to the J_1 – J_2 chain model based on the HTSE in the range of 100–350 K using $g = 2.11$ yields $J_1 = -61(2)$ K, $J_2 = 41(2)$ K, and $\chi_0 = 1.2(2) \times 10^{-5} \text{ cm}^3 \text{ mol}^{-1}$. This estimation for J_1 and J_2 , however, may not be reliable, because the HTSE is applicable only at high temperatures, while χ_0 must be reliable. In contrast, ED calculations can simulate χ down to lower temperatures: our full diagonalization for $N = 18$ spins in the periodic boundary condition using the ALPS package[39] may be reliable down to $T \sim 0.4J_2$. Assuming $\chi_0 = 1.2 \times 10^{-5} \text{ cm}^3 \text{ mol}^{-1}$ from the HTSE fit, we have obtained a best fit to the experimental data at $J_1 = -51$ K and $J_2 = 36$ K ($J_1/J_2 = -1.4$). χ values compared with a series of calculations for $J_1/J_2 = -1.4$, -0.7 , and 0 are shown in the inset of Fig. 2. We can determine the J_1 and J_2 almost uniquely to reproduce the whole χ .

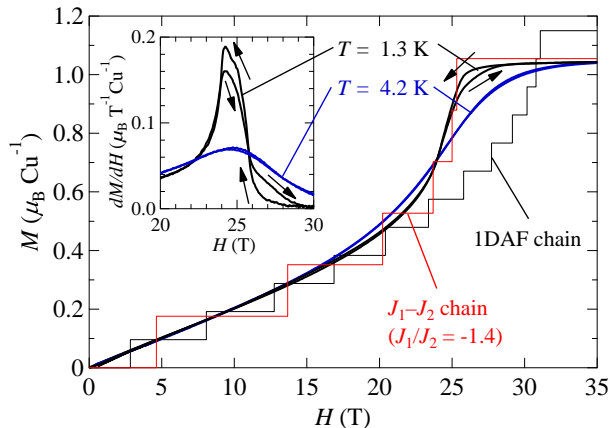


FIG. 4. (Color online) Magnetization curves recorded at 1.3 K (black curve) and 4.2 K (blue curve) upon increasing and then decreasing magnetic field in short magnetic pulses of a few milliseconds. An aggregate of small crystals with random orientation was used for each measurement. The stepwise black line shows a calculated magnetization curve for a uniform 1DAF chain with $J = 24.4$ K and $g = 2.30$, and the red one is for a frustrated J_1 - J_2 chain with $J_1 = -51$ K, $J_2 = 36$ K, and $g = 2.11$. Both calculations were performed by the Lanczos method for $N = 24$ sites. The inset shows the corresponding field-derivative curves near the saturation.

The heat capacity C is another important thermodynamic quantity that carries information about magnetic properties. The lattice contribution of $\text{NaCuMoO}_4(\text{OH})$ has been estimated from the heat capacity of $\text{NaZnMoO}_4(\text{OH})$. Taking into account a possible difference in the Debye temperature between the two compounds, the C - T curve of $\text{NaZnMoO}_4(\text{OH})$ has been expanded along the T axis by a factor of 1.07 so that the high-temperature parts above 150 K coincide between them. The magnetic contribution C_m is obtained by subtracting the expanded curve. C_m divided by temperature, C_m/T , which is shown in Fig. 3, exhibits a broad peak at 8 K, indicating the development of a short-range magnetic order, and then a sharp increase followed by a cusp at 0.59 K, which gives clear evidence of a long-range order. C_m/T down to low temperatures is not reproduced by ED calculations for a 1DAF chain with $J = 24.4$ K but for a J_1 - J_2 chain with the same J_1 and J_2 used in the χ fitting, which clearly demonstrates the reliability of our estimation. The transition temperature T_N of 0.59 K is as low as about 1% of J_2 , indicating a good one-dimensionality in magnetic interactions. Note that the one-dimensionality is better in the present compound than in LiCuVO_4 : the T_N of LiCuVO_4 is 2.1 K, which corresponds to about 5% of J_2 . Assuming that C_m/T decreases to 0 linearly below 0.5 K as expected from the high-temperature curve, the magnetic entropy S_m below T_N is estimated to be 0.15 J mol^{-1} , which is only 2.6% of the total entropy of $R \ln 2$ for spin 1/2. This confirms the good one-dimensionality of the present compound.

Magnetization measurements up to 50 T were performed to search for a spin nematic phase. Magnetization curves measured at 1.3 and 4.2 K are shown in Fig. 4, which are compared with those calculated by the Lanczos method for $N = 24$ sites using the ALPS package[39]. The small hysteresis in the magnetization curve may be due to a magnetocaloric effect under a quasi-adiabatic condition. The magnetization curve at 1.3 K rapidly increases at 23 T and almost saturates above 26 T, while the 4.2 K curve rises more gradually owing to thermal fluctuations. The saturation moment of $1.05 \mu_B/\text{Cu}$ is consistent with the g factor of 2.11(2). The calculated curve for the J_1 - J_2 chain model with the same parameters from the analyses of χ reproduces the 1.3 K curve very well, while that for the 1DAF chain does not. Note that the calculations assume $T = 0$, so that a thermal smearing effect should always be taken into account when compared with experiments. The saturation field H_s is calculated to be 25.4 T using the equation $H_s = \{J_1 + 3J_2 - J_2^2/(J_1 - J_2)\} k_B/(2g\mu_B)$ [3, 4], which is in good agreement with the experimental one.

In a single crystal of LiCuVO_4 , a linear variation in magnetization has been observed just below the saturation at 1.3 K, which may be associated with a spin nematic order[30]. Such a linear variation is not discernible in Fig. 4 for the present compound. The field derivatives of the magnetization curves at 1.3 K show asymmetric peaks at 24–25 T. This is partly because we used an aggregate of small crystals: an anisotropy in the g factor should cause a distribution in H_s so that a linear variation below H_s could be averaged to disappear. In addition, the measurement temperature of 1.3 K may not be low enough compared with $T_N = 0.59$ K to stabilize a spin nematic phase. Note that the temperature of 1.3 K is lower than $T_N = 2.1$ K for LiCuVO_4 . Further experiments using a large single crystal at temperatures as low as T_N are necessary to obtain evidence of the spin nematic phase in $\text{NaCuMoO}_4(\text{OH})$.

We have shown that $\text{NaCuMoO}_4(\text{OH})$ with $J_1 = -51$ K and $J_2 = 36$ K can be a good model compound for the J_1 - J_2 chain system. Let us compare $\text{NaCuMoO}_4(\text{OH})$ with the other model compounds listed in Table I. It is found in these compounds that J_2 does not change so much at 30–50 K, while $-J_1$ varies largely at 20–150 K. This is because J_2 occurs by the super-super exchange interaction via the Cu-O-O-Cu path, while J_1 by the superexchange interaction via the Cu-O-Cu path, only the latter of which is sensitive to local structures; J_1 becomes ferromagnetic when the Cu-O-Cu angle is close to 90° and changes into antiferromagnetic when the Cu-O-Cu angle exceeds 95 – 98° [40, 41]. For instance, a bond angle close to 90° leads to a large ferromagnetic J_1 of -138 K in $\text{Rb}_2\text{Cu}_2\text{Mo}_3\text{O}_{12}$, while the 95.0° bond angle of LiCuVO_4 gives $J_1 = -19$ K. In $\text{NaCuMoO}_4(\text{OH})$, two types of Cu-O-Cu path are present, one passing through O(1) with a 92.0° bond angle and the other passing through O(4) connected to hydrogen with a 103.7° bond angle (Fig. 1). The moderately large ferromagnetic

$J_1 = -51$ K may be attained from the dominant contribution of the Cu–O(1)–Cu path.

The good combination of J_1 and J_2 in NaCuMoO₄(OH) provides us with a better opportunity for studying the physics of the J_1 – J_2 chain. $H_s = 26$ T in NaCuMoO₄(OH) is much smaller than $H_s = 44.4$ T in LiCuVO₄, and is accessible in various experiments such as magnetization, NMR, and even neutron scattering experiments. One more important requirement for a good candidate compound is the availability of a large and clean single crystal. Among the compounds shown in Table I, large single crystals have been obtained only for PbCuSO₄(OH)₂[16–18], LiCu₂O₂[20–22], and LiCuVO₄[23–31]. However, “a cleanness” of these crystals seems unsatisfactory: a natural crystal of PbCuSO₄(OH)₂ is contaminated by impurities, and the two Li-containing crystals seem to suffer from Li deficiency or an interchange between Li and Cu atoms[24]. In contrast, NaCuMoO₄(OH) shows no such problems as the Na ion is much less mobile in crystals than the Li ion, and its large ionic radius prevents intersite mixing with Cu. Therefore, NaCuMoO₄(OH) can be an ideal compound for the J_1 – J_2 chain quantum magnet in various aspects. We continue our effort in obtaining a larger single crystal by

tuning growth conditions. In the future, we will clarify the physics of the J_1 – J_2 chain, particularly the nature of the spin nematic phase by ²³Na NMR experiments and others on sizable single crystals of NaCuMoO₄(OH).

In summary, we have investigated the magnetic susceptibility, heat capacity, and magnetization of the quasi-1D quantum antiferromagnet NaCuMoO₄(OH). By comparing them with those obtained using calculations by the exact diagonalization method, it is shown that NaCuMoO₄(OH) is a good candidate frustrated J_1 – J_2 magnet: $J_1 = -51$ K, $J_2 = 36$ K, $T_N = 0.59$ K, and $H_s = 26$ T (much smaller than 44.4 T for LiCuVO₄). Although our magnetization measurements at 1.3 K using an aggregate of small crystals have failed to obtain evidence of the spin nematic order, we think that our future experiments at lower temperatures using a large single crystal would uncover the intriguing physics of the frustrated J_1 – J_2 chain.

ACKNOWLEDGMENTS

We thank M. Koike and M. Isobe for chemical analyses and M. Takigawa, G. J. Nilsen, and H. Ishikawa for fruitful discussions.

-
- [1] H.-J. Mikeska and A. K. Kolezhuk, in *Quantum Magnetism*, ed. U. Schollwöck et al., Lecture Notes in Physics Vol. 645 (Springer-Verlag, Berlin, 2004) p. 1
- [2] L. Balents, *Nature* **464**, 199 (2010).
- [3] A. V. Chubukov, *Phys. Rev. B* **44**, 4693 (1991).
- [4] L. Kecke, T. Momoi, and A. Furusaki, *Phys. Rev. B* **76**, 060407 (2007).
- [5] T. Vekua, A. Honecker, H.-J. Mikeska, and F. Heidrich-Meisner, *Phys. Rev. B* **76**, 174420 (2007).
- [6] T. Hikihara, L. Kecke, T. Momoi, and A. Furusaki, *Phys. Rev. B* **78**, 144404 (2008).
- [7] J. Sudan, A. Lüscher, and A. M. Läuchli, *Phys. Rev. B* **80**, 140402 (2009).
- [8] M. E. Zhitomirsky and H. Tsunetsugu, *Europhys. Lett.* **92**, 37001 (2010).
- [9] M. Sato, T. Hikihara, and T. Momoi, *Phys. Rev. Lett.* **110**, 077206 (2013).
- [10] O. A. Starykh and L. Balents, *Phys. Rev. B* **89**, 104407 (2014).
- [11] H. T. Ueda and K. Totsuka, *cond-mat arXiv*, 1406.1960v1.
- [12] C. Dussarrat, G. C. Mather, V. Caignaert, B. Domenès, J. G. Fletcher, and A. R. West, *J. Solid. State Chem.* **166**, 311 (2002).
- [13] S.-L. Drechsler, O. Volkova, A. N. Vasiliev, N. Tristan, J. Richter, M. Schmitt, H. Rosner, J. Málek, R. Klingeler, A. A. Zvyagin, and B. Büchner, *Phys. Rev. Lett.* **98**, 077202 (2007).
- [14] S. F. Solodovnikov and Z. A. Solodovnikova, *J. Struct. Chem.* **38**, 765 (1997).
- [15] M. Hase, H. Kuroe, K. Ozawa, O. Suzuki, H. Kitazawa, G. Kido, and T. Sekine, *Phys. Rev. B* **70**, 104426 (2004).
- [16] H. Effenberger, *Mineral. Petrol.* **36**, 3 (1987).
- [17] A. U. B. Wolter, F. Lipps, M. Schapers, S.-L. Drechsler, S. Nishimoto, R. Vogel, V. Kataev, B. Buchner, H. Rosner, M. Schmitt, M. Uhlarz, Y. Skourski, J. Wosnitza, S. Sullow, and K. C. Rule, *Phys. Rev. B* **85**, 014407 (2012).
- [18] B. Willenberg, M. Schäpers, K. C. Rule, S. Süllow, M. Reehuis, H. Ryll, B. Klemke, K. Kiefer, W. Schottenhamel, B. Büchner, B. Ouladdiaf, M. Uhlarz, R. Beyer, J. Wosnitza, and A. U. B. Wolter, *Phys. Rev. Lett.* **108**, 117202 (2012).
- [19] S. E. Dutton, M. Kumar, M. Mourigal, Z. G. Soos, J.-J. Wen, C. L. Broholm, N. H. Andersen, Q. Huang, M. Zbiri, R. Toft-Petersen, and R. J. Cava, *Phys. Rev. Lett.* **108**, 187206 (2012).
- [20] R. Berger, A. Meetsma, and S. van Smaalen, *J. Less-Common. Met.* **175**, 119 (1991).
- [21] T. Masuda, A. Zheludev, B. Roessli, A. Bush, M. Markina, and A. Vasiliev, *Phys. Rev. B* **72**, 014405 (2005).
- [22] A. A. Bush, V. N. Glazkov, M. Hagiwara, T. Kashiwagi, S. Kimura, K. Omura, L. A. Prozorova, L. E. Svistov, A. M. Vasiliev, and A. Zheludev, *Phys. Rev. B* **85**, 054421 (2012).
- [23] M. A. Lafontaine, M. Leblanc, and G. Ferey, *Acta. Cryst.* **C45**, 1205 (1989).
- [24] A. V. Prokofiev, I. G. Vasilyeva, V. N. Ikorskii, V. V. Malakhov, I. P. Asanov, and W. Assmus, *J. Solid State Chem.* **177**, 3131 (2004).
- [25] M. Enderle, C. Mukherjee, B. Fåk, R. K. Kremer, J.-M. Broto, H. Rosner, S.-L. Drechsler, J. Richter, J. Malek, A. Prokofiev, W. Assmus, S. Pujol, J.-L. Raggazzoni, H. Rakoto, M. Rheinstädter, and H. M. Rønnow, *Europhys. Lett.* **70**, 237 (2005).

- [26] N. Büttgen, H. -A. Krug von Nidda, L. E. Stistov, L. A. Prozorova, A. Prokofiev, and W. Aßmus, *Phys. Rev. B* **76**, 014440 (2007).
- [27] T. Masuda, M. Hagihala, Y. Kondoh, K. Kaneko, and N. Metoki, *J. Phys. Soc. Jpn.* **80**, 113705 (2011).
- [28] M. Mourigal, M. Enderle, B. Fåk, R. K. Kremer, J. M. Law, A. Schneidewind, A. Hiess, and A. Prokofiev, *Phys. Rev. Lett.* **109**, 027203 (2012).
- [29] K. Nawa, M. Takigawa, M. Yoshida, and K. Yoshimura, *J. Phys. Soc. Jpn.* **82**, 094709 (2013).
- [30] L. E. Svistov, T. Fujita, H. Yamaguchi, S. Kimura, K. Omura, A. Prokofiev, A. I. Smirnov, Z. Honda, and M. Hagiwara, *JETP Lett.* **93**, 21 (2011).
- [31] N. Büttgen, K. Nawa, T. Fujita, M. Hagiwara, P. Kuhns, A. Prokofiev, A. P. Reyes, L. E. Svistov, K. Yoshimura, and M. Takigawa, submitted to *Phys. Rev. B*.
- [32] A. Moini, R. Peascoe, P. R. Rudolf, and A. Clearfield, *Inorg. Chem.* **25**, 3782 (1986).
- [33] M. M. Qurashi and W. H. Barnes, *Am. Mineral.* **39**, 416 (1954).
- [34] K. Kindo, S. Takeyama, M. Tokunaga, Y. H. Matsuda, E. Kojima, A. Matsuo, K. Kawaguchi, and H. Sawabe, *J. Low Temp. Phys.* **159**, 381 (2010).
- [35] N. Nakagawa, T. Yamada, K. Akioka, S. Okubo, S. Kimura, and H. Ohta, *Int. J. Infrared Millimeter Waves* **19**, 167 (1998).
- [36] D. C. Johnston, R. K. Kremer, M. Troyer, X. Wang, A. Klümper, S. L. Budko, A. F. Panchula, and P. C. Canfield, *Phys. Rev. B* **61**, 9558 (2000).
- [37] A. N. Vasil'ev, L. A. Ponomarenko, H. Manaka, I. Yamada, M. Isobe, and Y. Ueda, *Phys. Rev. B* **64**, 024419 (2001).
- [38] A. Bühler, N. Elstner, and G. S. Uhrig, *Eur. Phys. J. B* **16**, 475 (2000).
- [39] B. Bauer, L. D. Carr, H. G. Evertz, A. Feiguin, J. Freire, S. Fuchs, L. Gamper, J. Gukelberger, E. Gull, S. Gurtler, A. Hehn, R. Igarashi, S. V. Isakov, D. Koop, P. N. Ma, P. Mates, H. Matsuo, O. Parcollet, G. Pawłowski, J. D. Picon, L. Pollet, E. Santos, V. W. Scarola, U. Schollwöck, C. Silva, B. Surer, S. Todo, S. Trebst, M. Troyer, M. L. Wall, P. Werner, and S. Wessel, *J. Stat. Mech.* P05001 (2011); A. F. Albuquerque, F. Alet, P. Corboz, P. Dayal, A. Feiguin, S. Fuchs, L. Gamper, E. Gull, S. Gurtler, A. Honecker, R. Igarashi, M. Körner, A. Kozhevnikov, A. Läuchli, S. R. Manmana, M. Matsumoto, I. P. McCulloch, F. Michel, R. M. Noack, G. Pawłowski, L. Pollet, T. Pruschke, U. Schollwöck, S. Todo, S. Trebst, M. Troyer, P. Werner, and S. Wessel, *J. Magn. Magn. Mater.* **310**, 1187 (2007).
- [40] V. H. Crawford, H. W. Richardson, J. R. Wasson, D. J. Hodgson, and W. E. Hatfield, *Inorg. Chem.* **15**, 2107 (1976).
- [41] Y. Mizuno, T. Tohyama, S. Maekawa, T. Osafune, N. Motoyama, H. Eisaki, and S. Uchida, *Phys. Rev. B* **57**, 5326 (1998).